Andrzej Piotrowicz
AGH University of Science and Technology, Faculty of Non-Ferrous Metals, Department of Physical Chemistry and Metallurgy of Non-Ferrous Metals
30 Mickiewicz Av., Krakow, 30-059 Poland, andpio@agh.edu.pl

Stanisław Pietrzyk
AGH University of Science and Technology, Faculty of Non-Ferrous Metals, Department of Physical Chemistry and Metallurgy of Non-Ferrous Metals
30 Mickiewicz Av., Krakow, 30-059 Poland

DISSOLUTION OF MANGANESE (IV) OXIDE FROM TANTALUM CAPACITOR SCRAP BY ORGANIC ACIDS

Abstract
The dissolution of MnO_2 from tantalum capacitor scrap using organic acids in various process conditions was studied. The initial materials were of two types: LTC (leaded tantalum capacitors) and SMDTC (surface-mounted device tantalum capacitors). The research materials were prepared by pyrolysis, grinding and sieving and the preparation processes were characterized. Dissolution of MnO_2 was carried out with the use of sulfuric acid solutions with the addition of acetic, ascorbic, citric and oxalic organic acids. Results show that the addition of organic acids significantly improves dissolution yields (72-94 vs 90-99 % for H_2SO_4 and acid mixtures, respectively). In practice, a concentration of organic acid above 1 M results in the complete removal of MnO_2.

Key words
tantalum capacitors, tantalum recycling, eco-friendly recycling, transition metals recovery

Introduction
The publication of a list of critical raw materials for the European Union (EU) [1, 2] shows that tantalum is one of them. Tantalum has many uses, such as for heat exchange, as a superalloy additive, for sputtering and others, but the most important use is for tantalum capacitors (TC) which are characterized by a high electrical capacity. TCs are crucial for the development of the high-tech electrical/electronic industry, especially for the manufacture of portable devices and energy control and storage systems. Tantalum is mostly imported to the EU, and recycling of this metal is poorly developed in the EU – therefore, scientific efforts should be made to increase tantalum recycling efficiency.
A tantalum capacitor essentially consists of three components:
- an internal tantalum sinter covered with manganese(IV) oxide, graphite and silver with tantalum wire, hereinafter referred to as an anode,
- an outer layer of epoxy resin
- electrical leads, metal pads and solders.

Figure 1 shows a schematic of an anode. The metallic tantalum powder is sintered with tantalum wire – the whole is a sinter covered with the following layers: tantalum(V) oxide (Ta_2O_5), manganese(IV) oxide (MnO_2), graphite, metallic silver and epoxy resin. Metallic tantalum powder is a substrate for the production of a dielectric layer – Ta_2O_5. The use of powder increases the surface area, which in turn increases the electrical capacity. MnO_2 is a cathode and silver provides chemical protection. To prevent undesirable reactions between the cathode and silver, there is a graphite layer between them. Epoxy resin containing halogens increase the decomposition temperature and serves as a mechanical protection and electrical insulation [3,4].
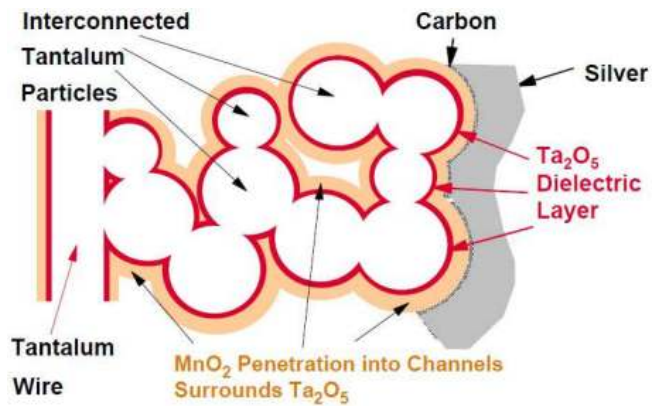
Figure 1. Schematic representation of the structure of a tantalum capacitor and the cathode connecting layers (the whole is encapsulated in epoxy resin and is a three-dimensional structure, no electrical leads are marked)
Source: [3]

There are two types of TCs (Figure 2):
- leaded tantalum capacitors (LTC) and
- surface-mounted device tantalum capacitors (SMDTC).

Despite the differences in the external structure, which results from the mounting method to the electric circuit (though-hole or surface-mounted technology), the internal structure is almost identical (Figure 3).

Figure 2. Tantalum capacitor scraps used in this work – LTC (right) and SMDTC (left)
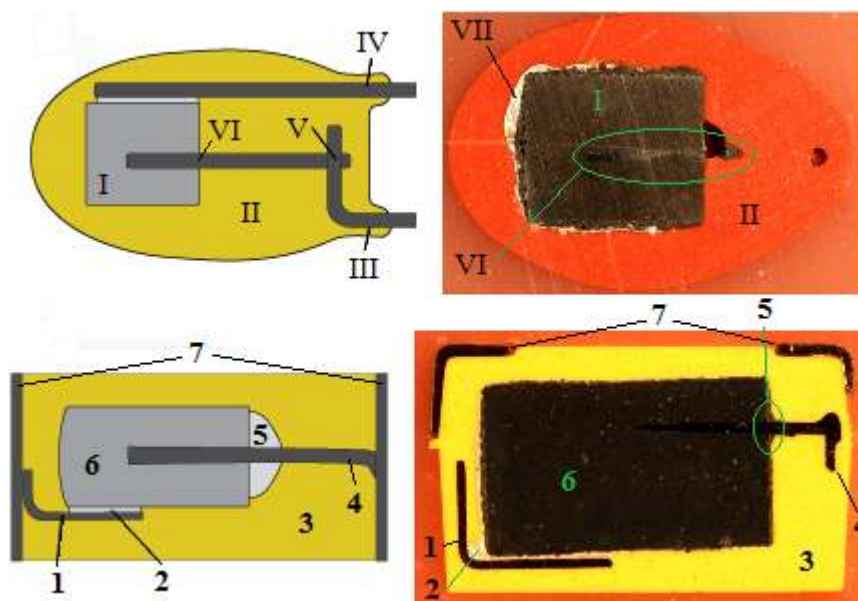*Source: the Author's own materials*

Figure 3. LTC and SMDTC schemes (left side at the top and at the bottom) and optical images of a section through the internal structure of LTC and SMDTC (right side at the top and at the bottom): I, 6 - anode; II, 3 - epoxy resin encapsulant; III - positive lead; IV - negative lead; V – weld; VI, 4 – anode wire; VII – silver paint; 1 and 7 – lead frames; 2 - silver filled epoxy; 5 - teflon washer
Source: [5] and Author's materials (optical images)

Tantalum recycling from capacitor scraps

Many studies of recycling tantalum from scrap electric and electronic equipment show that it is possible to effectively recover tantalum by various piro- and/or hydrometallurgical methods such as: mechanical-magnetic separation and alkali/acid treatment [6], tantalum solubility in a Cu-Fe alloy [7], chlorination of tantalum by iron chlorides [8,9,10], chemical reduction of oxidized tantalum [10,11], recovery with ionic liquids [12], supercritical water treatment [13], steam gasification with sodium hydroxide [14], vacuum pyrolysis [15,16] and others. This work [17] strictly concerns the removal of MnO_2 from manganese material, which may be a tantalum capacitor with hydrochloric acid or a mixture of sulfuric acid and hydrogen peroxide. Both methods cause either the emission of dangerous compounds ($MnCl_4$, and hence, chlorine), or are long-term (over twelve hours). In the authors' previous work [11], the possibility of tantalum recycling through the reduction of oxidized anodes (consisting mainly of Ta_2O_5) by magnesium was studied. Incomplete manganese removal can contaminate the end product, giving phases with Ta, oxygen and a reducing agent (Figure 4), thus lowering the efficiency of the reduction process. Therefore, before tantalum oxide reduction, it is necessary to remove the Mn.
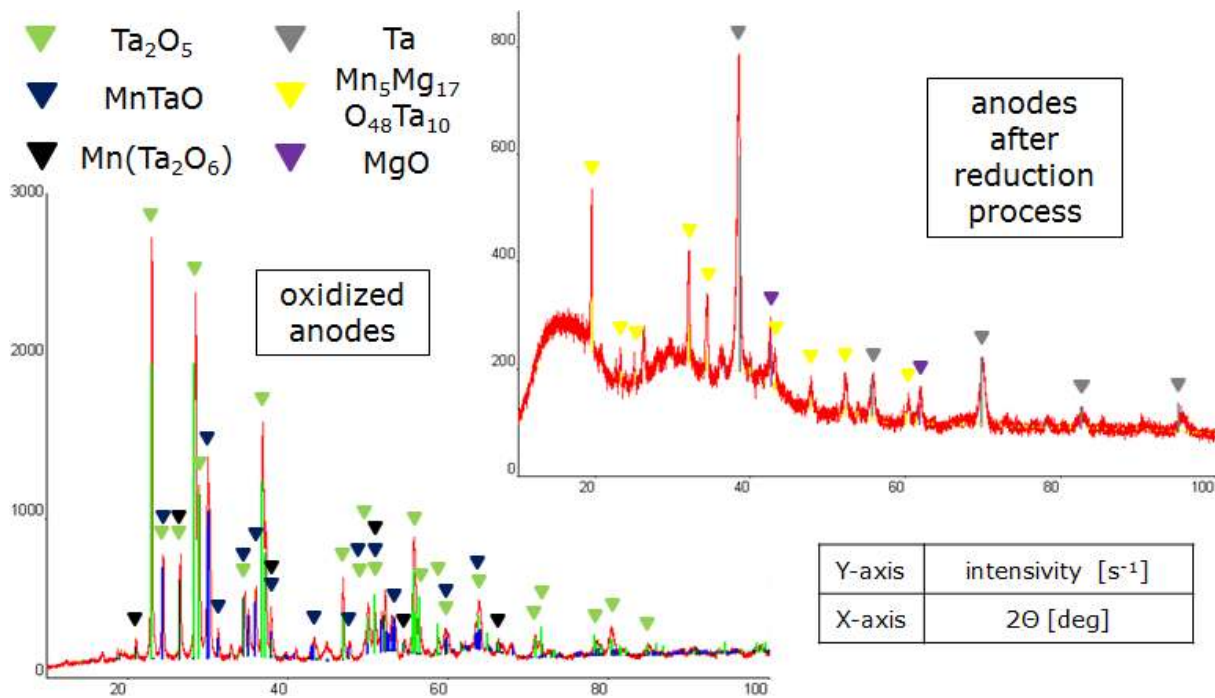
Figure 4. X-ray diffraction analyses of the oxidized anodes before and after thermal reduction by magnesium (left and right, respectively); apart from the MgO and metallic tantalum, in the end product there are also manganese-containing phases (reflection peaks under the yellow markers)
Source: based on [11]

Dissolution of manganese (IV) oxide in organic acid solutions

The dissolution kinetics of manganese oxides in sulfuric acid is described by Gudunov et al. and Artanomona et al. [18,19]. Chen et.al. [17] presented the results of a study on the removal of MnO_2 from TC by reducing the leaching reaction of $H_2SO_4 + H_2O_2$ and hydrochloric acid (HCl) + H_2O_2. Studies on dissolving MnO_2 by using H_2SO_4 also containing organic acids (OA) such as oxalic [19,20], ascorbic and citric acids [20] have been carried out. Manganese removal occurs by reducing leaching, in which the OAs are used as the reducing agents. In comparison to removing Mn only by H_2SO_4, the addition of OA improves the removal efficiency [20].

Objective

The objective was to study the possibility of removing MnO_2 from TC scrap by a dissolution process in the following sulfuric and organic acid solutions: acetic ($C_2H_4O_2$), ascorbic ($C_6H_8O_6$), citric ($C_6H_8O_7$) and oxalic ($C_2H_2O_4$). A series of laboratory tests were carried out to determine the optimal conditions and parameters such as acid concentration, duration, temperature and liquid-to-solid ratio. After the hydrometallurgical treatment, the end product was expected to obtain a manganese-free tantalum concentrate.

Materials from two types of tantalum capacitor scraps were used: LTC and SMDTC which were appropriately prepared by pyrolysis, grinding and sieving. Each of these steps was described and parametrized.

Experiment

The research plan is presented in Figure 5. Initial materials were LTC and SMDTC scraps from a domestic source. For a determination of the contents of the components, which are conventionally divided into epoxy resin, electrical components (electrical leads and lead frames) and anodes (a source of Ta and Mn), some part of the scraps were dismantled and the mass fractions were calculated.
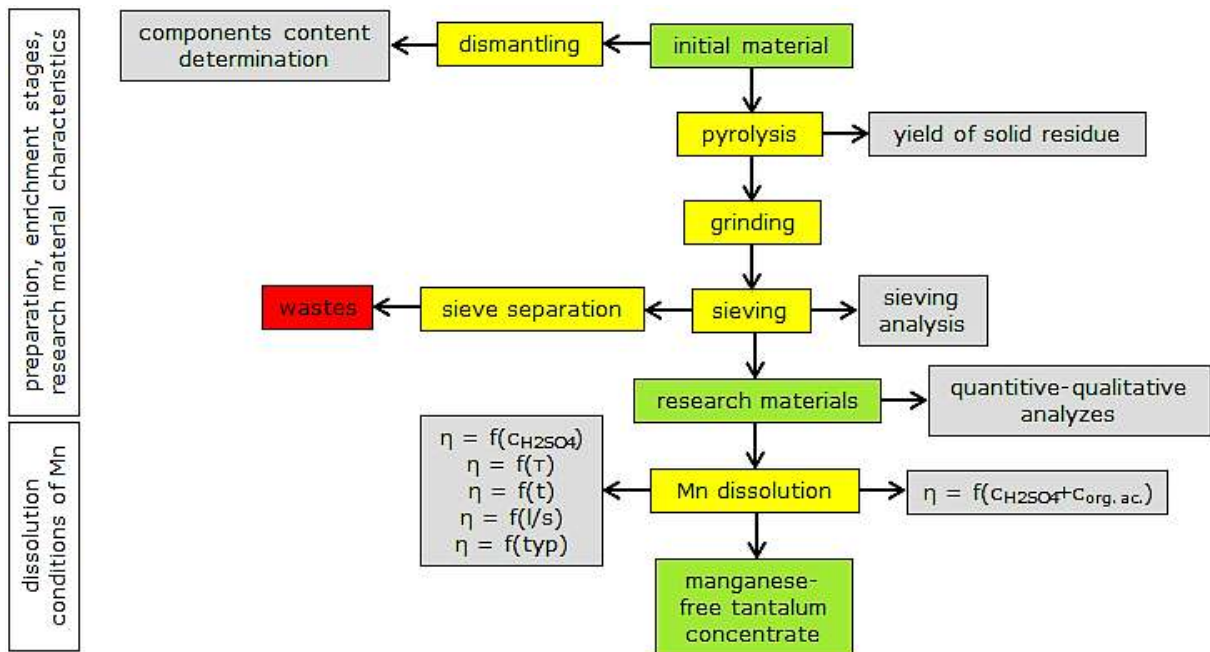
Figure 5. Diagram of the present research: green – research materials, yellow – study steps, grey – analyses and calculations
Source: Author's materials

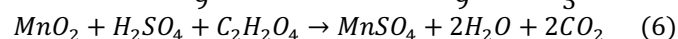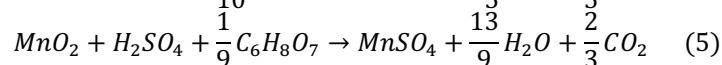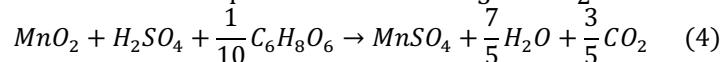For research purposes, both types of capacitors were prepared separately in the following order:
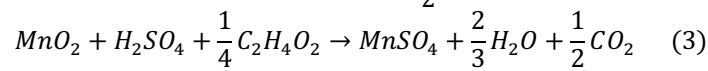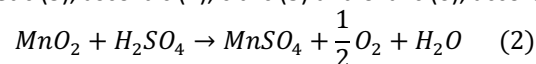
- first, capacitor scraps were pyrolized in an electric furnace at 400 ^{0}C in a nitrogen atmosphere (99.2%) for 45 min;
- after this, the solid residues were grinded in a laboratory grinding machine for 5 min;
- finally, the grinded materials were manually sieved on square mesh sieves for 10 min and some parts such as electrical components were separated.

The aim of the pyrolysis was the removal of most of the epoxy resin, other volatile carbon compounds and halogens without changing the oxidation state of other components, such as Ta and Mn. Waste materials, such as electrical leads and lead frames were removed by sieving. The yield of solid residue (R), which was used to evaluate the pyrolysis process, is given according to the formula [15]:

$$R = \frac{m_{SR}}{m_{IM}} \cdot 100\% \quad (1)$$

where: m_{SR} – the mass of solid residue after pyrolysis, m_{IM} – the mass of initial material, both in g. Sieve analysis was performed on the basis of particle size distribution and the average particle size was calculated. Some particle-size classes, which were later treated as waste were discarded, and the rest, which was the appropriate research material for the dissolution study of manganese, was subjected to quantitative and qualitative analyses. The content of elements was determined by an energy dispersive X-ray fluorescence analysis (EDXRF, MiniPal4 PANalytical) and X-ray powder diffraction analysis (XRD, Rigaku Miniflex II).

Laboratory tests of MnO_2 dissolution were carried out by leaching using solutions of H_2SO_4 (95 %) with/without the following OAs (99.5 %): acetic (3), ascorbic (4), citric (5) and oxalic (6), according to reactions [18-20]:

$$MnO_2 + H_2SO_4 \rightarrow MnSO_4 + \frac{1}{2}O_2 + H_2O \quad (2)$$

$$MnO_2 + H_2SO_4 + \frac{1}{4}C_2H_4O_2 \rightarrow MnSO_4 + \frac{2}{3}H_2O + \frac{1}{2}CO_2 \quad (3)$$

$$MnO_2 + H_2SO_4 + \frac{1}{10}C_6H_8O_6 \rightarrow MnSO_4 + \frac{7}{5}H_2O + \frac{3}{5}CO_2 \quad (4)$$

$$MnO_2 + H_2SO_4 + \frac{1}{9}C_6H_8O_7 \rightarrow MnSO_4 + \frac{13}{9}H_2O + \frac{2}{3}CO_2 \quad (5)$$

$$MnO_2 + H_2SO_4 + C_2H_2O_4 \rightarrow MnSO_4 + 2H_2O + 2CO_2 \quad (6)$$

The quantities of the OAs were stoichiometric in relation to H_2SO_4 according to the chemical equations. The acid solutions were heated with a laboratory hot plate (Figure 6). After reaching the given temperature, the research material was added into the beaker. Mixing speed was 200 rpm. After the reaction time had elapsed, the mixture

was filtered through a glass funnel; the solid residue was rinsed with distilled water and 92 % ethanol. A composition analysis was performed for this solid residue. The dissolution yield (η) was determined by the formula:

$$\eta_x = \frac{C_{x,0} - C_{x,\tau}}{C_{x,\tau}} \cdot 100\% \quad (7)$$

where: $C_{x,0}$ – initial concentration (x is element), $C_{x,\tau}$ – concentration after the process (both in %) - determined by EDXRF analysis.
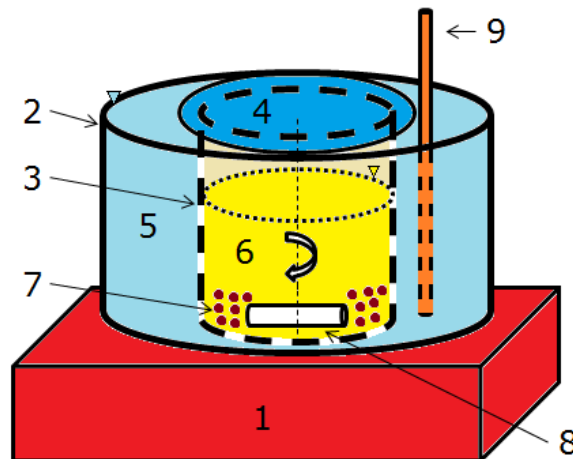

Figure 6. Scheme of apparatus for dissolution study: 1 – hot plate, 2 –bath, 3 – beaker, 4 – watch glass, 5 – water, 6 – acids solution, 7 – research material, 8 – magnetic stirrer, 9 – thermocouple
Source: Author's materials

Results

Table 1 shows the components' mass fractions of initial materials. The anode is a significant part of the capacitors (± 40 and 58 % for SMDTC and LTC, respectively). In SMDTC, the share of epoxy resin and anode was more or less similar, but electrical components had a large share. The presented mass fractions are not universal; they concern only the TC scrap in this work.

Table 1. Component mass fractions of the TCs used in this study

capacitor type	epoxy resin	electrical leads/metal pads and lead frames	anode
		wt [%] (±0.1)	
LTC	37.1	5.1	57.8
SMDTC	36.9	23.2	39.9

Source: Author's materials

The pyrolized materials retained their original shape, however became black due to the coke content (Figure 7). Yields of the solid residue of pyrolysis (R), depending of the type of TC, are presented in Table 2. Although this parameter value for SMDTC can be compared with literature data [15,16] and corresponds with them, there is no data for LTC. The higher R for SMDTC can be explained by the high quality of epoxy resin (more silicon and halogens).
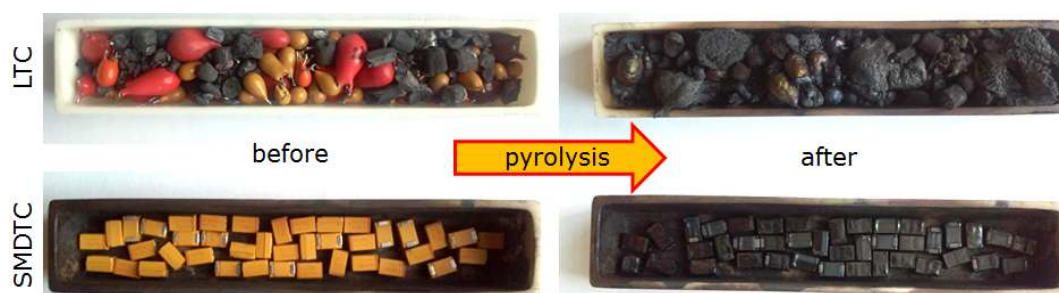

Figure 7. Materials' appearance before and after pyrolysis process
Source: Author's materials

Table 2. Yields of solid residue after the pyrolysis process

capacitor type	mass of initial material m_{IM}	mass of solid residue after pyrolysis m_{SR}	yield of solid residue R
	[g] (±0.001)		[%] (±0.1)
LTC	139.492	122.812	88.0
SMDTC	16.678	15.848	95.0

Source: Author's materials

Figure 8 shows the fractions obtained after grinding and sieving. Fractions >0.4 mm and 0.315-0.4 mm were electrical leads and tantalum wires – their longitudinal shape and the fact that they do not grind easily, enabled their easy separation. Fractions <0.315 mm, representing 92-99 %, were a fine powder – these fractions constitute the research material for testing the Mn dissolution. Figure 9 shows the particle size classes, particle size distribution and cumulative curve, on the basis of which the average particle size was determined to be 0.127 and 0.055 mm for LTC and SMDTC, respectively.

Figure 8. Fractions of pyrolized and ground tantalum capacitors
Source: Author's

The chemical compositions of research material are presented in Table 3. While in LTC the main component is tantalum, in SMDTC it is SiO_2. There was much SiO_2, MnO_2 and solder elements in the LTC, as well as Cu in SMDTC. The materials also included Fe and Ni from partially ground electric leads and metal pads. Elements and components such as Pb, Sn, Cu and perovskites may have come not so much from the TC as from the entire electrical scrap from which they originated.
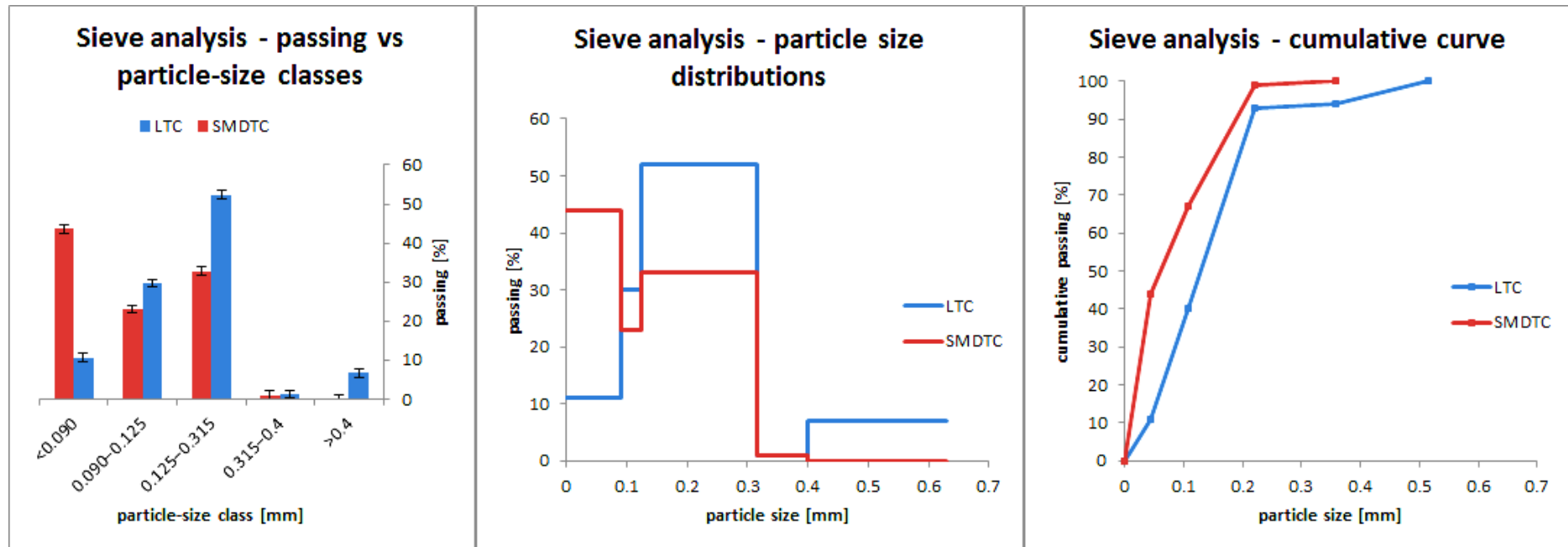
Figure 9. Sieve analysis of pyrolized and ground tantalum capacitors: on the left – particle-size classes in passing function, in the middle – particle size distributions, on the right – cumulative curve

Source: Author's materials

Table 3. Chemical compositions of research material for dissolution study – results of EDXRF and XRD analyses; the carbon content is not included, the Ta content has been converted to Ta_2O_5

	SiO_2	MnO_2	Fe	Ni	Cu	Ag	Ta_2O_5	Sn	Pb	TiO_2	BaO	CaO
source	epoxy resin	catode	electric leads and lead frames		silver layer		wire, sinter and dielectric	solder		perovskites		
type	wt [%]											
LTC	13.50	13.54	3.08	0.45	nd	6.41	39.10	14.71	8.28	0.607	0.40	nd
SMDTC	33.24	12.87	3.58	0.12	19.61	6.83	22.41	nd	nd	0.690	nd	0.65

Source: Author's materials

In any case, it was observed that, during the dissolution studies, a part of the material floated on the free surface. This was most likely hydrophobic silica and pyrolytic coke particles. After leaching, the filtrate took on a light flesh color (Mn ions presence). Fe, Ni and Cu, as well as Mn, were simultaneously dissolved (although it was not a priority) and dissolution yields of these elements are also included (Table 4). Analysis of the effect of H_2SO_4 concentration on dissolution yields (Figure 10A) showed that both Mn, Fe and Ni pass into solution at low c_{H2SO4}. In the cases of Mn and Fe, the equilibrium is set at c_{H2SO4} about 2 mol·l^{-1} and in the case of Ni – at a lesser acid concentration of about 1 mol·l^{-1}. The effect of time on η_{Mn} is insignificant (Figure 10B); for τ = 180 min and more, η_{Mn} reached a maximum value. In the range of 60-120 min, a significant increase in η_{Fe} was observed, and almost after 120 min, most of the Fe dissolved. As shown in Figure 10C, in the temperature range of 30-60 ^{0}C η_{Mn} was constant; in the whole temperature range η_{Fe} was high. In the studied l/s (Figure 10D), this parameter had no effect on the η_{Mn}. The highest value of η_{Fe} was reached for l/s = 20 ml·g^{-1}. Figure 10E shows the dissolution yield depended on the type of capacitor (LTC or SMDTC). In the case of SMDTC the results were lower. This is due to the fact that the acid also reacts with Cu. Based on the above results, subsequent tests with the addition of an organic acid on the dissolution yield were carried out at the following constant parameters: τ = 120 min, t = 30 ^{0}C, l/s = 20 ml·g^{-1} and for LTC.

Table 4. Element contents and dissolution yields data depending on process parameters, a dissolution study with only H_2SO_4

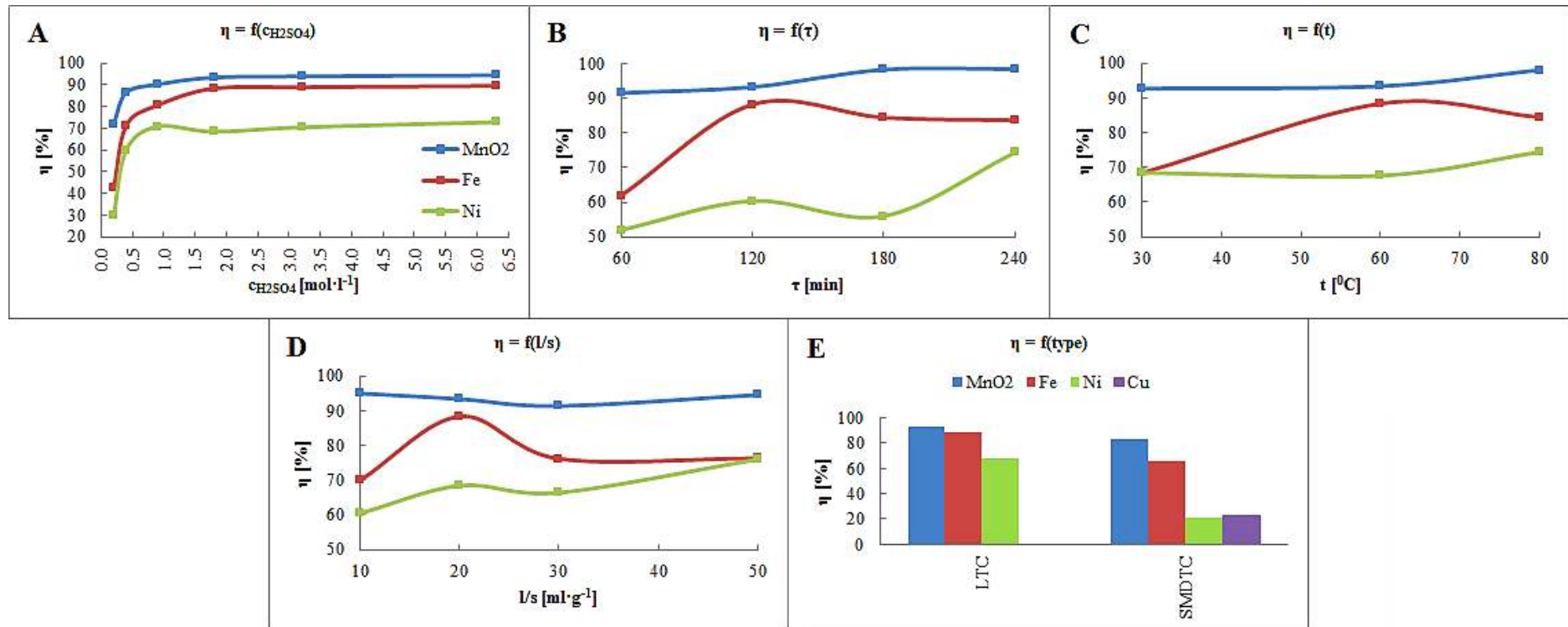| parameter	constant parameters		MnO$_2$		Fe		Ni		Cu	
			wt, %	η, %	wt, %	η, %	wt, %	η, %	wt, %	η, %
c_{H2SO4}, mol·l^{-1}	▪ τ = 120 min ▪ t = 30 ^{0}C ▪ l/s = 20 ml·g^{-1} ▪ RM = LTC	0.2	3.80	71.9	1.78	42.3	0.32	30.0		
		0.4	1.84	86.4	0.89	71.2	0.18	60.0		
		0.9	1.33	90.2	0.60	80.6	0.13	70.8		
		1.8	0.90	93.4	0.36	88.3	0.14	68.4		
		3.2	0.83	93.9	0.34	88.9	0.13	70.4		
		6.3	0.76	94.4	0.32	89.5	0.12	72.8		
τ, min	▪ c_{H2SO4} = 1.8 mol·l^{-1} ▪ t = 30 ^{0}C ▪ l/s = 20 ml·g^{-1} ▪ RM = LTC	60	1.13	91.6	1.17	62.0	0.22	52.0		
		120	0.90	93.4	0.36	88.3	0.18	60.4		
		180	0.22	98.4	0.48	84.5	0.20	56.0		
		240	0.19	98.6	0.50	83.7	0.12	74.4		
t, ^{0}C	▪ c_{H2SO4} = 1.8 mol·l^{-1} ▪ τ = 120 min ▪ l/s = 20 ml·g^{-1} ▪ RM = LTC	30	1.00	92.6	0.98	68.3	0.14	68.4		
		60	0.90	93.4	0.36	88.3	0.15	67.6		
		80	0.27	98.0	0.48	84.4	0.12	74.4		
l/s, ml·g^{-1}	▪ c_{H2SO4} = 1.8 mol·l^{-1} ▪ τ = 120 min ▪ t = 30 ^{0}C ▪ RM = LTC	10	0.68	94.9	0.93	69.9	0.18	60.4		
		20	0.90	93.4	0.36	88.3	0.14	68.4		
		30	1.17	91.3	0.73	76.1	0.15	66.4		
		50	0.74	94.5	0.73	76.3	0.11	76.0		
capacitor type, -	▪ c_{H2SO4} = 1.8 mol·l^{-1} ▪ τ = 120 min ▪ t = 30 ^{0}C ▪ l/s = 20 ml·g^{-1}	LTC	0.90	93.4	0.36	88.3	0.14	68.4		
		SMDTC	2.17	83.1	1.21	66.1	0.10	21.4	17.94	22.8

Source: Author's

Figure 10. Effect on dissolution yields of MnO₂, Fe and Ni: A - H₂SO₄ concentration, B - time, C - solid/liquid ratio, D - temperature, E - capacitor type; based on the data in Table 5
Source: Author's materials

Table 5 shows the results of reductive leaching by use of the following OAs: $C_2H_4O_2$ (Figure 11A), $C_6H_8O_6$ (Figure 11B), $C_6H_8O_7$ (Figure 11C) and $C_2H_2O_4$ (Figure 11D) respectively. In almost all cases, the equilibrium of manganese dissolution was set at an acid concentration of about 1 M, except for the $C_2H_2O_4$, where already at 0.2 M η_{Mn} it reached a constant value. Maximum η_{Mn}, in comparison to leaching with H_2SO_4 only, was almost always higher. Therefore, due to the very good results of manganese dissolution in the entire concentration range, it is recommended to use low concentrations of this acid, especially, so that the solubility of $C_2H_2O_4$ in the aqueous solutions is lowest in comparison with the other OAs. Dissolution yields of iron for $C_2H_4O_2$ and $C_6H_8O_7$ were similar to those of leaching with H_2SO_4 only. The lower η_{Fe} values were in the case of using $C_6H_8O_6$, where the equilibrium was set for the whole range of concentration. Whereas the situation was different when using $C_2H_2O_4$: η_{Fe} and η_{Ni} (also for $C_6H_8O_6$) decreased with increased concentration. The reason for this is the very low solubility of the formed nickel citrate, iron and nickel oxalates. As in the case of only H_2SO_4, the additional use of OAs results did not give η_{Ni} results higher than 80 %. However, it should be noted that the nickel concentration in the initial material was very low (0.45 %).

Table 5. Element contents and dissolution yields data depending on process parameters, a dissolution study with H_2SO_4 and organic acids solutions; organic acid concentrations are stoichiometric in relation to H_2SO_4 according to reactions (3-6)

organic acid	constant parameters	$c_{OA.}$, mol·l^{-1}	MnO$_2$		Fe		Ni	
			wt, %	η, %	wt, %	η, %	wt, %	η, %
$C_2H_4O_2$	τ = 120 min, t = 30 °C, l/s = 20 ml·g^{-1}, RM = LTC	0.2	1.27	90.6	0.73	76.4	0.13	70.4
		0.4	1.04	92.3	0.53	82.9	0.13	72.0
		0.9	0.60	95.5	0.54	82.3	0.13	70.8
		1.8	0.45	96.7	0.48	84.5	0.12	73.6
		3.2	0.30	97.8	0.35	88.6	0.11	76.4
$C_6H_8O_6$		0.2	1.37	89.9	0.90	70.6	0.20	56.0
		0.4	1.07	92.1	0.87	71.6	0.17	61.6
		0.9	0.13	99.1	0.79	74.3	0.17	61.2
		1.8	0.28	97.9	0.77	75.1	0.20	56.6
		3.2	0.43	96.8	0.74	76.1	0.22	52.0
$C_6H_8O_7$		0.2	1.42	89.5	0.91	70.3	0.20	56.0
		0.4	1.17	91.3	0.83	73.1	0.17	62.4
		0.9	0.46	96.6	0.49	84.0	0.15	67.2
		1.8	0.42	96.9	0.38	87.6	0.14	69.2
		3.2	0.37	97.3	0.27	91.2	0.13	71.2
$C_2H_2O_4$		0.2	0.19	98.6	0.48	84.4	0.13	70.8
		0.4	0.22	98.4	0.58	81.2	0.12	72.8
		0.9	0.24	98.2	0.82	73.4	0.16	64.0
		1.8	0.24	98.2	1.00	67.5	0.17	62.0
		3.2	0.25	98.2	1.18	61.8	0.18	60.0

Source: Author's
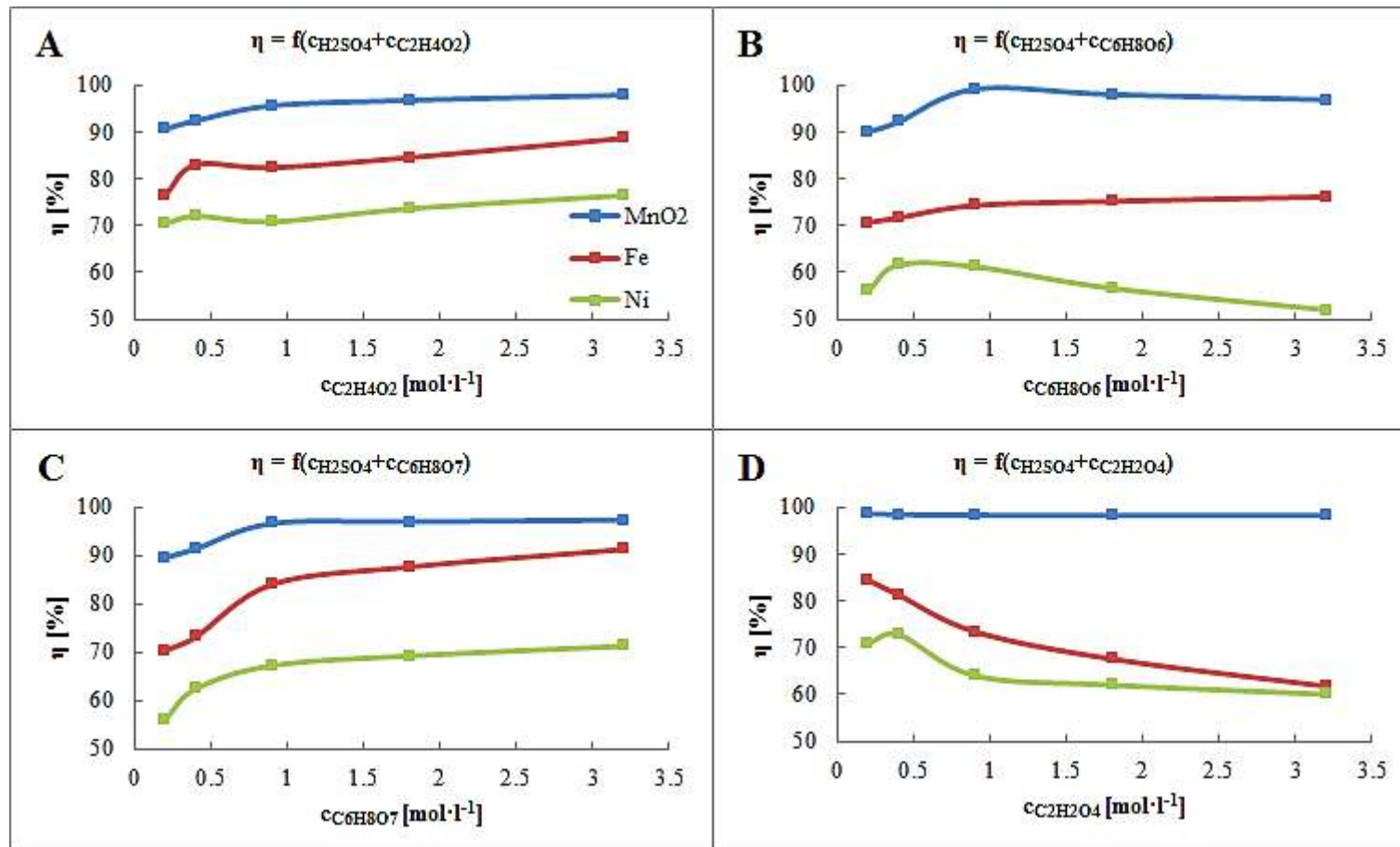
Figure 11. Effect of organic acid concentration on dissolution yields of MnO₂, Fe and Ni: A - $C_2H_4O_2$, B - $C_6H_8O_6$, C - $C_6H_8O_7$, D - $C_2H_2O_4$; based on the data in Table 5
Source: Author's materials

Application of manganese dissolution in tantalum recycling

Figure 12 shows the potential use of manganese in the development of a tantalum recycling method based on literature and this work. The process of manganese removal by a hydrometallurgical method enables the convenient treatment of a solution for the recovery of manganese salts or oxides, which are widely used in industry and organic acid regeneration. Although organic acids can pose a threat to health or life (especially corrosive/toxic acetic and oxalic acids; ascorbic and citric acids are generally considered harmless), they are safer than mineral acids, and their utilization is not a major challenge. Many stages of tantalum material enrichment have been considered: from sorting and dismantling to electrostatic separation. Their use enables the removal of ballast components such as coke and silica, thereby increasing the tantalum content and manganese in the concentrate. As regards the recovery of copper and silver, some studies [11,21] have indicated that the best solution for silver removal is nitric acid; leaching with sulfuric acid in the presence of H_2O_2 is not so effective [21]. There is a possibility of collective leaching of Mn, Cu and Ag, however, subsequent stages of separation of individual elements are required. If selective leaching is used, a portion of nitric acid can be replaced by a safer and environmentally friendly mixture of H_2SO_4 and OA. Material that contains only tantalum after the removal of contaminated materials such as manganese and other ferrous materials provides a good base for magnesiothermic reduction.
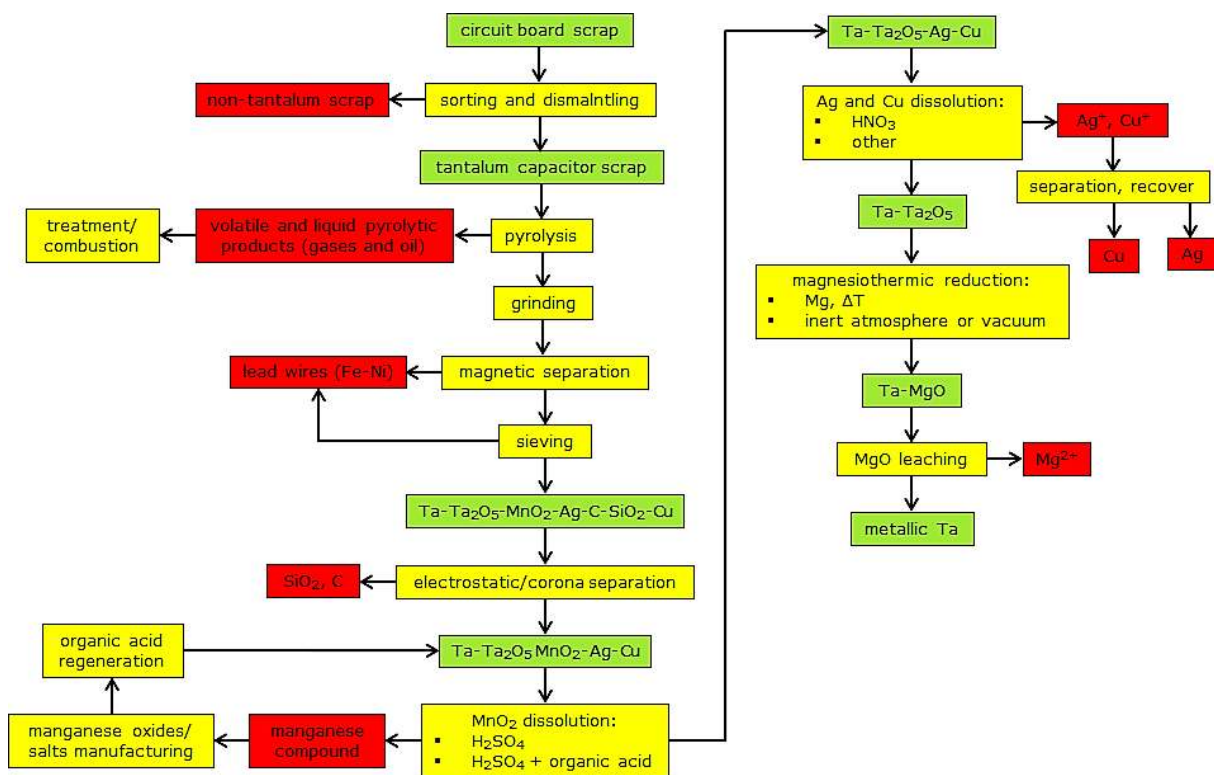

Figure 12. A proposition for the use of manganese dissolution in the process of recycling tantalum from scrap electrical/electronic equipment : green – containing-tantalum material (main stream), yellow – a process stage, red – a secondary valuable material or waste; this includes the steps of the enrichment process (mechanical, magnetic, electrostatic), hydro- and pyrometalurgical processes and regeneration and recovery of valuable materials
Source: based on [6,10,11,15,16] and this work

Summary and conclusions

A tantalum capacitor is a complex electronic subassembly in terms of structure and composition with an epoxy resin encapsulant, terminals and anode. The anode has a multi-layered three-dimensional structure and consists of metallic tantalum (sinter and wire), Ta_2O_5 (dielectric layer), MnO_2 (cathode), graphite (anti-diffusion layer) and silver (chemical protection). Moreover, in leaded capacitor scrap may be tin and lead, derived from the solder, and in the capacitor to surface-mounted technology there may be contaminates derived from perovskite-based dielectrics. All together this means that tantalum recycling from scrap capacitors is a challenge.

Pre-treatment processes, such as pyrolysis, grinding and sieving, are good methods for the enrichment of tantalum concentrate originating from scrap for hydrometallurgical treatment. The material remaining after

these processes is a powder, devoid of some part of the resin, as well as most of the iron and nickel. The obtained research materials contained significant amounts of silica (13.5-33 %) and manganese (about 13 %), which are impurities, and high tantalum concentrations (22-39 %).

Manganese removal based on its dissolution in sulfuric acid is an effective method, although the addition of organic acids, such as $C_2H_4O_2$, $C_6H_8O_6$, $C_6H_8O_7$ and $C_2H_2O_4$ increases the dissolution yield. In the studied ranges of process parameters, such as acid concentration, time, temperature and solid/liquid ratio, the optimal parameters were: τ = 120 min, t = 30 ^{0}C, l/s = 20 ml·g^{-1}. Additionally, iron and nickel can simultaneously be removed with manganese. The effect of the addition of organic acid on the dissolution yield is significant, otherwise a lower concentration of acids is required. Exceptionally high η_{Mn} were observed in the cases of $C_6H_8O_7$ and $C_2H_2O_4$. However, in the latter case, a decrease of η_{Mn} relative to iron and nickel was noted along with an increase of acid concentration.

The use of manganese dissolution can be implemented to the tantalum recycling process. Due to the lack of manganese, subsequent stages of tantalum recycling may be more effective. In addition, the manganese dissolution in a mixture of sulfuric and organic acids is selective, i.e. metals such as silver can be leached and recovered in another processing step.

References
[1]   Communication from The Commission to The European Parliament, The Council, The European Economic and Social Committee and The Committee of The Regions - Tackling The Challenges in Commodity Markets and on Raw Materials 2.2.2011, https://eur-lex.europa.eu/legal-content/EN/TXT/PDF/?uri=CELEX:52011DC0025&from=EN, 11.02.2018
[2]   Communication from The Commission to The European Parliament, The Council, The European Economic and Social Committee and The Committee of The Regions - on the 2017 list of Critical Raw Materials for the EU 13.9.2017, https://eur-lex.europa.eu/legal-content/EN/TXT/PDF/?uri=CELEX:52017DC0490&from=EN, 11.02.2018
[3]   J.D. Prymak, New tantalum capacitors in power applications, The 1998 IEEE 5 (1998) 1129-1137
[4]   J. Gill, Technical information - basic tantalum capacitor technology, AVX Ltd., Tantalum Division, https://escies.org/download, 11.02.2018
[5]   High temperature epoxies increase the service range of tantalum capacitors, https://www.masterbond.com/techtips/high-temperature-epoxies-increase-service-range-tantalum-capacitors, 11.20.2018
[6]   M. Yoshida, K. Matsuzaki, T. Aoki, R. Ishii, Method for recovering tantalum. Mitsui Mining and Smelting Co Ltd, United State of America. Patent application publication, US2013/0014611 A1, Priority date 01.04.2010, Publication date 17.01.2013
[7]   R. Kikuchi, T. Yamamato, M. Nakamoto, Preliminary information of laboratorial tantalum recovery and considerations for a potential solution for conflict mineral and wildlife conservation, Environ. Nat. Resour. Res. 4(1) (2014) 31-38
[8]   K. Mineta, T.H. Okabe, Recycling process for tantalum from capacitor scraps and chlorination by using chloride wastes, Shigen-to-Sozai 121(7) (2005) 284-290
[9]   B. Niu, Z. Chen, Z. Xu, Method for recycling tantalum from waste tantalum capacitors by chloride metallurgy, ACS Sustainable Chem. Eng. 5(2) (2017) 1376-1381
[10]   R. Matsuoka, K. Mineta, T.H. Okabe, Recycling process for tantalum and some other reactive metal scraps, Proceedings of the Symposium on Solid and Aqueous Waste from Non-ferrous Metal Industries, Charlotte: TMS, 2004, 689-696
[11]   A. Piotrowicz, S. Pietrzyk, Tantalum recycling from waste of electrical and electronic equipment, SEED 2016, E3S Web Conf. 10(74) (2016) 1-4
[12]   L. Spitczok von Brisinski, D.I.D. Goldmann, P.F. Endres, Recovery of metals from tantalum capacitors with ionic liquids, Chem. Ing. Tech. 86(1-2) (2014) 196-199
[13]   B. Niu, Z. Chen, Z. Xu, Recovery of tantalum from waste tantalum capacitors by supercritical water treatment, ACS Sustainable Chem. Eng. 5(5) (2017) 4421-4428
[14]   S. Katano, T. Wajima, H. Nakagome, Recovery of tantalum sintered compact from used tantalum condenser using steam gasification with sodium hydroxide, APCBEE Procedia 10 (2014) 182-186
[15]   B. Niu, Z. Chen, Z. Xu, Recovery of valuable materials from waste tantalum capacitors by vacuum pyrolysis combined with mechanical–physical separation, ACS Sustainable Chem. Eng. 5(3) (2017) 2639-2647

[16] B. Niu, Z. Chen, Z. Xu, Vacuum pyrolysis characteristics and parameter optimization of recycling organic materials from waste tantalum capacitors, Journal of Hazardous Materials 342 (2018) 192-200

[17] V.M. Orlov, E.N. Kiselev, Leaching of manganese dioxide from porous bodies, Russian Journal of Applied Chemistry 85(11) (2012) 1699-1702

[18] E.B. Godunov, A.D. Izotov, I.G. Gorichev, Dissolution of manganese oxides of various compositions in sulfuric acid solutions studied by kinetic methods, Inorg. Mat. 54(1) (2018) 67-71

[19] I.V. Artamonova, I.G. Gorichev, E.B. Godunov, Kinetics of manganese oxides dissolution in sulphuric acid solutions containing oxalic acid, Engineering 5 (2013) 714-719

[20] W.S. Chen, C.T. Liao, K.Y. Lin, Recovery zinc and manganese from spent battery powder by hydrometallurgical route, Energy Procedia 107 (2017) 167-174

[21] A. Piotrowicz, S. Pietrzyk, Study on dissolution conditions of manganese oxide and silver from tantalum capacitors scrap, Zrozumieć Naukę 2 (2018) 181-196